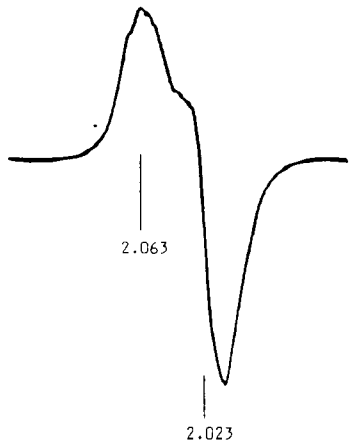

Figure 3. EPR powder spectrum of $Fe_6S_5(\mu\text{-SPh})(P\text{-}n\text{-}Bu_3)_4(SPh)_2$ at 77 K.

pounds $[Fe_6S_6(PEt_3)_4(SR)_2]$ in which quasi-reversible reductions at more negative values (−0.87 V for R = Ph and −0.60 V for R = p-C_6H_4Br) were observed that more nearly approach chemical reversibility.[18]

^{1}H NMR. The downfield ^{1}H NMR spectrum of **1** in $CDCl_3$ at room temperature is shown in Figure 2. The line widths of protons are broadened and isotropically shifted due to the paramagnetic nature of the iron atoms. Comparison with cluster **3** showed that two types of thiophenolato ligands are present in compound **1**, two as terminal ligands and one as a bridge. On the other hand, with one additional electron for the iron atoms in compound **1**, the isotropic shifts of protons decreased as compared to **3**, substantiating the decreased paramagnetic nature of **1**, which agrees well with the result of the EPR study ($S = {}^1/_2$). When **1** is converted to **2** by reacting it with acylchloride, all the absorptions downfield for the thiophenolate protons disappeared, including the bridging thiophenolate protons, with only the n-butyl protons remaining upfield (see Experimental Section).

EPR. The EPR spectrum of cluster **1** was measured at 77 K and is shown in Figure 3. It exhibits a strong axial symmetry with the two components at $g = 2.063$ and $g = 2.023$. This observation is consistent with a polynuclear system $[Fe_6S_5{}^*S]^+$ where the metal ions are antiferromagnetically coupled to yield a ground state spin of $S = {}^1/_2$ as in the $[Fe_6S_6]^{3+}$ cluster core.[9] The $S = {}^1/_2$ ground state in the former occurred from the combination of formal integral oxidation states one Fe(III) + five Fe(II) where one high-spin ferric ion ($3d^5$, $S = {}^5/_2$) and five high-spin ferrous ions ($3d^6$, $S = 2$) couple with one another to give the $S = {}^1/_2$ ground state.

Acknowledgment. We acknowledge the grants from the NNSF of China and Natural Science Foundation of The Chinese Academy of Sciences in support of this research. We wish to express our gratitude to the chemical analysis group of this Institute. We thank also Prof. Y. T. Wang for assistance with the Mössbauer measurement.

Supplementary Material Available: Tables of atomic positional and thermal parameters, bond distances and bond angles, and calculated hydrogen atom positions for $Fe_6S_5(\mu\text{-SPh})(P\text{-}n\text{-}Bu_3)_4(SPh)_2$ (9 pages); a listing of calculated and observed structure factors (16 pages). Ordering information is given on any current masthead page.

Contribution from the Department of Chemistry, Leiden University, P.O. Box 9502, 2300 RA Leiden, The Netherlands, Department of Crystallography, Catholic University, Toernooiveld, 6525 ED Nijmegen, The Netherlands, and Dipartimento di Chimica, Università di Siena, 53100 Siena, Italy

A Unique Bromo- and Thioether-Bridged Tetranuclear Mixed-Valence Copper(I)–Copper(II) Compound with the N,S-Donor Ligand 4-((Ethylthio)methyl)-5-methylimidazole

E. Bouwman,[†] W. L. Driessen,*[,†] J. Reedijk,[†] C. Smykalla,[‡] J. M. M. Smits,[‡] P. T. Beurskens,[‡] F. Laschi,[§] and P. Zanello[§]

Received June 12, 1990

The mixed-valence compound tribromo[4-((ethylthio)methyl)-5-methylimidazole]copper(II)copper(I), $Cu_2(C_7H_{12}N_2S)Br_3$, forms spontaneously from an ethanol solution of copper(II) bromide and the ligand. The complex crystallizes as dark brown needles in the monoclinic space group $I2/a$: $a = 13.6953$ (15) Å, $b = 12.4347$ (5) Å, $c = 15.7589$ (7) Å, $\beta = 91.960$ (11)°, $Z = 8$, $R = 0.038$, and $R_w = 0.045$ for 1902 observed reflections. Each copper(II) ion is surrounded by a nitrogen atom at 1.964 (5) Å, a thioether sulfur at 2.350 (2) Å, and two bromide ions at 2.439 (1) and 2.394 (1) Å, in a square-planar geometry. The copper(I) ion is surrounded by three bromide ions at 2.360 (1), 2.483 (1), and 2.573 (1) Å and one thioether sulfur at 2.321 (2) Å in a distorted tetrahedral geometry. The dinuclear asymmetric unit is held together by a double bromide bridge between the Cu(I) and Cu(II) ion; the third bromide is terminally bonded to the Cu(I) at 2.360 (1) Å. The Cu(I) ion in each asymmetric unit is connected to the Cu(II) ion in another dinuclear unit through the bridging thioether sulfur of the ligand, thereby forming a unique tetranuclear species. The bromide, which is terminally bonded to the Cu(I), is a distance of 3.073 (1) Å from the nearest Cu(II), which is regarded as semicoordinating. Through this bond all tetranuclear species are bromide bridged to one another, forming a polymer with the copper(II) in a square-pyramidal environment. In confirmation of its mixed-valence nature, the title compound undergoes one-electron oxidation as well as one-electron reduction in DMSO at rather positive, coincident potential values ($E^{\circ\prime}$ = +0.19 V vs SCE). X-ray, electrochemical, and EPR techniques point to an electron-localized $Cu^{II}Cu^{I}$ species.

Introduction

The couple Cu(II)–Cu(I) plays a central role in biological electron-transfer processes, since copper ions are integral parts of the active sites of many proteins involved in redox processes.[1,2] The architecture of the active site determines the specific function: a distorted tetrahedral N_2SS^* environment in the (blue) type I copper proteins like plastocyanin[3] and azurin[4] for electron transfer; a dinuclear $(N_3Cu)_2$ site in heamocyanin[5] (type III) for dioxygen

[†] Leiden University.
[‡] Catholic University.
[§] Università di Siena.

(1) Adman, E. T. *Top. Mol. Struct. Biol.* **1985**, *6*, 1.
(2) Huber, R. *Angew. Chem.* **1989**, *28*, 848.
(3) Colman, P. M.; Freeman, H. C.; Guss, J. M.; Murata, M.; Norris, V. A.; Ramshaw, J. A. M.; Venkatappa, M. P. *Nature* **1978**, *272*, 319.
(4) Norris, G. E.; Anderson, B. F.; Baker, E. N. *J. Am. Chem. Soc.* **1986**, *108*, 2784.
(5) Volbeda, A.; Hol, W. G. J. *J. Mol. Biol.* **1989**, *209*, 249.

0020-1669/90/1329-4881$02.50/0

transfer; a distorted-square-planar N_4 environment in the type II copper protein superoxide dismutase[6] for the removal of O_2^-. All three types are present in ascorbate oxidase[2,7] whereby the type II and the type III sites form a new trinuclear site. The nitrogen donor atoms involved in the binding of the copper in these active sites are invariably imidazole nitrogens from histidine residues. The sulfur atoms involved are thioether sulfurs from methionine or thiolate sulfurs from cysteine. To model copper active sites, azole nitrogens and thioether sulfurs are used as functional groups in polydentate chelating ligands.[8-10] Although a perfect mimic of one of the active sites of copper proteins has not yet been reported, the coordination chemistry that results from these modeling efforts is extremely rich with a large variety of different copper environments.[8]

The ligand 4-((ethylthio)methyl)-5-methylimidazole (memi), which is an NS-donor ligand eventually suitable for modelling an N_2S_2 environment, forms coordination compounds with several transition-metal salts.[11] The copper(II) fluoroborate and nitrate compounds of memi are catalytically active in the oxidation of 2,6-dimethylphenol to poly(phenylene oxide) and diphenoquinone.[12] In this reaction, the copper species switches between the +1 and +2 oxidation states. In the search for other active memi compounds, copper halides were also used. The reaction product of memi with copper(II) bromide rendered a compound in which half the copper appeared to be copper(I). The characterization, structurally, spectroscopically, and electrochemically, of this mixed-valence compound is presented in this paper. In this connection it must be taken into account that electrochemistry is quite commonly used to characterize mixed-valent dicopper species,[13,14] of which few have also been X-ray characterized.[15,16]

Experimental Section

The synthesis of the ligand 4-((ethylthio)methyl)-5-methylimidazole (memi) has been described elsewhere.[17] The mixed-valence copper coordination compound was prepared by dissolving copper(II) bromide (1 mmol) in 5 mL of ethanol and adding this solution to a solution of the ligand memi (1 mmol) in 25 mL of warm ethanol. After filtration of the hot reaction mixture, the complex started to crystallize on cooling. The solution was kept open to air to ensure slow evaporation of the solvent, thereby enlarging the crop of dark brown crystals. Anal. Found (calcd) for $Cu_2Br_3C_7H_{12}N_2S$: Cu, 23.7 (24.3); C, 16.5 (16.07); H, 2.28 (2.31); N, 5.37 (5.36); S, 6.22 (6.13).

Metal analyses were carried out complexometrically with Na_2H_2edta as the complexing agent. CHN analysis was performed in the Microanalytical Laboratory in Dublin.

Magnetic susceptibilities of solid samples were measured on a Faraday balance.

Conductance measurements of a 10^{-3} mol dm^{-3} sample in DMSO were performed at room temperature with an ORION Model 990101 cell assembly connected to a Model 101 conductivity meter.

Infrared spectra in the 4000–180-cm^{-1} range of the samples pelleted in KBr were recorded on a Perkin-Elmer spectrophotometer, equipped with a PE data station.

Table I. Atomic Coordinates and Equivalent Isotropic Thermal Parameters (Å^2 × 100) with Esd's of the Non-Hydrogen Atoms of $Cu_2(C_7H_{12}N_2S)Br_3$

atom	x	y	z	U(eq)
Cu(1)	−0.15831 (9)	0.53532 (8)	−0.27749 (7)	4.62 (4)
Cu(2)	−0.11926 (8)	0.80854 (7)	−0.30441 (5)	3.54 (3)
Br(3)	−0.09652 (6)	0.37240 (6)	−0.22066 (5)	4.43 (3)
Br(4)	−0.11534 (7)	0.65261 (5)	−0.39814 (4)	4.22 (2)
Br(5)	−0.12133 (6)	0.69761 (5)	−0.18030 (4)	4.00 (2)
C(10)	−0.1179 (6)	1.0625 (5)	−0.2845 (4)	3.62 (20)
N(11)	−0.1225 (5)	1.0086 (5)	−0.5127 (3)	4.35 (20)
C(12)	−0.1243 (6)	0.9096 (6)	−0.4776 (4)	4.07 (23)
N(13)	−0.1247 (5)	0.9178 (4)	−0.3944 (3)	3.49 (18)
C(14)	−0.1221 (5)	1.0263 (5)	−0.3754 (4)	3.12 (19)
C(15)	−0.1208 (5)	1.0841 (5)	−0.4483 (4)	3.69 (22)
C(16)	−0.1156 (7)	1.2011 (6)	−0.4631 (6)	5.6 (3)
C(17)	−0.1430 (8)	1.0693 (7)	−0.0773 (5)	5.8 (3)
C(18)	−0.1123 (6)	0.9675 (5)	−0.1208 (4)	4.24 (23)
S(19)	−0.17253 (12)	0.95513 (11)	−0.22403 (9)	2.98 (4)

Electronic spectra (28000–5000 cm^{-1}) were recorded on a Perkin-Elmer 330 spectrophotometer, also equipped with a PE data station, in DMSO solution or as a solid in standard reflectance mode.

EPR measurements were carried out with an ER 200-SRCB Bruker spectrometer operating at X-band frequency (9.78 GHz). The external magnetic field was calibrated with a microwave bridge Model ER 041 MR Bruker wavemeter and the temperature was controlled with a Model ER 4111 VT Bruker device with accuracy of ±1%.

Cyclic voltammetry was performed in a three-electrode cell with a platinum working electrode surrounded by a platinum-spiral counter electrode and an aqueous saturated calomel electrode (SCE) mounted with a Luggin capillary as the reference electrode. The apparatus used for direct current voltammetry at the platinum electrode with periodical renewal of the diffusion layer has been described elsewhere.[18] Either a BAS 100A electrochemical analyzer or a multipurpose Amel instrument (a Model 566 analog function generator and a Model 552 potentiostat) were used as polarizing units. Controlled-potential coulometric tests were performed in an H-shaped cell with anodic and cathodic compartments separated by a sintered glass disk. The working macroelectrode was a platinum gauze; a mercury pool was used as the counter electrode. The Amel potentiostat was associated to an Amel Model 558 integrator. Under the present experimental conditions the ferrocenium–ferrocene couple was located at +0.40 V.

Data Collection and Structure Refinement. A single crystal of approximate dimensions 0.07 × 0.10 × 0.22 mm, mounted in a glass capillary, was used for data collection. Cell dimensions were determined from reflections with $11° < \theta < 64°$. Intensity data were collected for 19966 reflections (half a sphere up to $\theta = 70°$, with $h = 0$–16, $k = 0$–15, and $l = -19$ to +19), the drift-correction curve showed an intensity decrease to 7%, due to decomposition. The semiempirical absorption correction factors (EMPABS[19]) were in the range 0.67–1.00; the second empirical absorption correction (DIFABS[19]) ranged from 0.63 to 1.90. Of the 2478 unique reflections, 1986 were observed ($R_{merge} = 0.056$). The structure was solved by automated Patterson and direct methods. The position of the Cu and Br atoms were located from the Patterson map (PATSYS[19]) and automatically used as input for DIRDIF,[19] which gave the positions of all non-hydrogen atoms in one run. Hydrogen atoms were placed at a calculated distance of 1.00 Å of their parent atoms. During refinement the hydrogen atoms, with a fixed isotropic thermal parameter of 7.2 (Å^2 × 100), were coupled to their parent atoms.

Least-squares refinement (SHELX86[19]): weight factor = 0.0004, shift over esd ratio less than 0.12. $R = 0.038$, $R_w = 0.045$ for 1902 observed reflections, with $F_o > 6\sigma(F_o)$, and 150 variables. Final difference Fourier peaks were less than 0.72 e Å^{-3}. Geometrical data were obtained with the program PARST.[19]

Crystal data for $Cu_2Br_3C_7H_{12}N_2S$: $M_r = 523.05$, monoclinic, $a = 13.6953$ (15) Å, $b = 12.4347$ (5) Å, $c = 15.7589$ (7) Å, $\beta = 91.960$ (11)°, $V = 2682.1$ (3) Å^3, λ(Cu Kα) = 1.5418 Å, $T = 293$ K, space group $I2/a$, $Z = 8$, $D_c = 2.591$ g cm^{-3}, μ(Cu Kα) = 157.11 cm^{-1}, $F(000) = 1976$.

The fractional coordinates of the non-hydrogen atoms of Cu_2(memi)Br_3 are listed in Table I. Bond distances and bond angles of the non-hydrogen atoms are given in Table II. Lists of the atomic coordinates of the hydrogen atoms, of the non-hydrogen anisotropic thermal

(6) Bailey, D. B.; Ellis, P. D.; Fee, J. A. *Biochemistry* **1981**, *19*, 591.
(7) Messerschmidt, A.; Rossi, A.; Ladenstein, R.; Huber, R.; Bolognesi, M.; Gatti, G.; Marchesini, A.; Petruzzelli, R.; Finazzo-Agro, A. *J. Mol. Biol.* **1989**, *206*, 513.
(8) Bouwman, E.; Driessen, W. L.; Reedijk, I. *Coord. Chem. Rev.* **1990**, *104*, 143–172.
(9) van Rijn, J.; Bouwman, E.; Empfield, J. R.; Driessen, W. L.; Reedijk, J. *Polyhedron* **1989**, *8*, 1965.
(10) Haanstra, W. G.; Driessen, W. L.; Reedijk, J.; Turpeinen, U.; Hämäläinen, R. *J. Chem. Soc., Dalton Trans.* **1989**, 2309.
(11) Bouwman, E.; Westheide, C. E.; Driessen, W. L.; Reedijk, J. *Inorg. Chim. Acta* **1989**, *166*, 291.
(12) Tullemans, A. H. J.; Bouwman, E.; de Graaff, R. A. G.; Driessen, W. L.; Reedijk, J. *Recl. Trav. Chim. Pays-Bas* **1990**, *109*, 70.
(13) Zanello, P.; Tamburini, S.; Vigato, P. A.; Mazzocchin, G. A. *Coord. Chem. Rev.* **1987**, *77*, 165.
(14) Bond, A. M.; Haga, M.; Creece, I. S.; Robson, R.; Wilson, J. C. *Inorg. Chem.* **1989**, *28*, 559 and references therein.
(15) Dunaj-Jurco, M.; Ondrejovic, G.; Melnik, M.; Garaj, J. *Coord. Chem. Rev.* **1988**, *83*, 1 and references therein.
(16) Agnus, Y.; Gisselbrecht, J. P.; Louis, R.; Metz, B. *J. Am. Chem. Soc.* **1989**, *111*, 1494.
(17) Bouwman, E.; Driessen, W. L. *Synth. Commun.* **1988**, *18*, 1581.
(18) Zanello, P.; Bartocci, C.; Maldotti, A.; Traverso, O. *Polyhedron* **1983**, *2*, 791.
(19) Smits, J. M. M.; Behm, H.; Bosman, W. P.; Beurskens, P. T. *J. Crystallogr. Spectrosc. Res.* **1988**, *18*, 447 and references therein.

Table II. Bond Lengths (Å) and Bond Angles (deg) Involving the Non-Hydrogen Atoms of $Cu_2(C_7H_{12}N_2S)Br_3$[a]

Cu(1)-Br(3)	2.360 (1)	C(10)-C(14)	1.501 (8)
Cu(1)-Br(4)	2.483 (1)	N(11)-C(12)	1.350 (9)
Cu(1)-Br(5)	2.573 (1)	N(11)-C(15)	1.382 (9)
CU(1)-S(19)′	2.321 (2)	C(12)-N(13)	1.315 (8)
Cu(2)-Br(4)	2.439 (1)	N(13)-C(14)	1.382 (8)
Cu(2)-Br(5)	2.394 (1)	C(14)-C(15)	1.357 (8)
Cu(2)-S(19)	2.350 (2)	C(15)-C(16)	1.476 (9)
Cu(2)-N(13)	1.964 (5)	C(17)-C(18)	1.506 (9)
C(10)-S(19)	1.816 (6)	C(18)-S(19)	1.806 (6)
Br(3)″-N(11)	3.624 (5)	Cu(2)-Br(3)‴	3.0725 (14)
Br(3)-Cu(1)-Br(4)	134.70 (6)	Cu(1)-Br(4)-Cu(2)	89.57 (4)
Br(3)-Cu(1)-BE(5)	112.74 (5)	Cu(1)-Br(5)-Cu(2)	88.47 (4)
Br(4)-Cu(1)-Br(5)	87.02 (4)	C(14)-C(10)-S(19)	106.06 (41)
Br(4)-Cu(2)-Br(5)	92.17 (4)	C(12)-N(11)-C(15)	108.51 (54)
Br(4)-Cu(2)-N(13)	96.53 (15)	N(11)-C(12)-N(13)	109.85 (59)
Br(5)-Cu(2)-N(13)	170.90 (16)	Cu(2)-N(13)-C(12)	131.69 (46)
Br(4)-Cu(2)-S(19)	163.07 (7)	Cu(2)-N(13)-C(14)	121.24 (39)
Br(5)-Cu(2)-S(19)	89.66 (5)	C(12)-N(13)-C(14)	106.93 (52)
N(13)-Cu(2)-S(19)	81.25 (16)	C(10)-C(14)-N(13)	120.01 (51)
Br(3)-Cu(1)-S(19)′	112.65 (6)	C(10)-C(14)-C(15)	130.44 (56)
Br(4)-Cu(1)-S(19)′	103.93 (6)	N(13)-C(14)-C(15)	109.51 (52)
Br(5)-Cu(1)-S(19)′	97.46 (6)	N(1)-C(15)-C(14)	105.20 (55)
Cu(1)-S(19)′-C(10)′	113.40 (22)	N(11)-C(15)-C(16)	123.60 (61)
Cu(1)-S(19)′-C(18)′	114.34 (23)	C(14)-C(15)-C(16)	131.18 (62)
Cu(1)-S(19)′-Cu(2)′	111.95 (8)	C(17)-C(18)-S(19)	110.76 (51)
Br(3)‴-Cu(2)-N(13)	85.8 (15)	Cu(2)-S(19)-C(10)	98.42 (21)
Br(3)‴-Cu(2)-S(19)	92.6 (6)	Cu(2)-S(19)-C(18)	114.23 (24)
Br(3)‴-Cu(2)-Br(4)	104.0 (5)	C(10)-S(19)-C(18)	103.06 (31)
Br(3)‴-Cu(2)-Br(5)	94.7 (4)		

[a] Key: single prime, $^1/_2 - x$, $^1/_2 - y$, $^1/_2 - z$; double prime, $+x$, $^1/_2 - y$, $^1/_2 + z$; triple prime, $-x$, $^1/_2 + y$, $^1/_2 - z$.

parameters, and of the observed and calculated structure factors are available as supplementary material.

Results and Discussion

General Data. The dark brown compound $Cu_2(memi)Br_3$ was obtained from the reaction of memi with copper(II) bromide. Its stoichiometry was inferred from the elemental analyses. The pattern of the absorption bands of the solid compound in the infrared resembled strongly the infrared pattern of the free ligand, indicating the presence of the intact ligand. Some of the bands were shifted or split as a result of coordination. The diffuse reflectance spectrum shows an extremely broad band around 15.3 $\times 10^3$ cm^{-1}, apparently due to charge-transfer transitions from imidazole, from bromide, and/or from sulfur to copper with the relatively weak d–d transition obscured by these bands.[20-22] This band is most likely not due to intervalence transitions as the solid-state structure is consistent with valence-localized Cu centers and as the electrochemistry and EPR studies suggest a strongly localized electronic structure (see below).

In the solid state, $Cu_2(memi)Br_3$ is paramagnetic, with a magnetic moment corresponding to one unpaired spin ($\mu_{eff} = 1.85$ μ_B per dimeric unit). In DMSO the compound behaves as a nonelectrolyte.

Description of the Structure of $[Cu_2(memi)Br_3]_\infty$. A PLUTO[23] projection of the asymmetric unit with the atomic labeling is given in Figure 1. The asymmetric unit $Cu_2(memi)Br_3$ is held together by a double bromide bridge between Cu(1) and Cu(2) with the third bromide terminally bonded to Cu(1). The Cu(1)–Cu(2) distance is 3.468 (1) Å. The angle between the planes Br(4)–Cu(1)–Br(5) and Br(4)–Cu(2)–Br(5) is 162.16 (5)°. This rather flat dinuclear fragment lies parallel to the *bc* plane. Cu(1) is surrounded by three bromide ions at 2.360 (1), 2.483 (1), and 2.573 (1) Å and one thioether sulfur at 2.321 (2) Å in a distorted

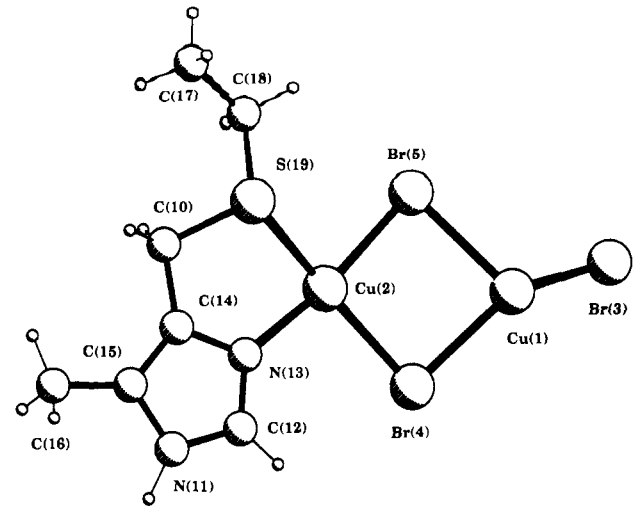

Figure 1. Asymmetric unit of $Cu_2(memi)Br_3$ with the atomic labeling.

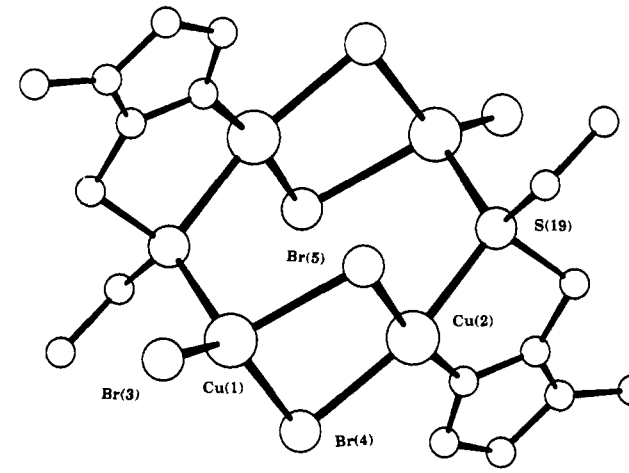

Figure 2. Tetrameric unit of $Cu_2(memi)Br_3$.

tetrahedral geometry, with angles ranging between 87° and 134.7°. Cu(2) is surrounded by a nitrogen atom at 1.964 (5) Å and a thioether sulfur at 2.350 (2) Å of the ligand memi and two bromide ions at 2.439 (1) and 2.394 (1) Å, in a square-planar geometry. A third bromide is at an axial site with a distance of 3.073 (1) Å, which is considered as semicoordinating. Another bromide at 3.554 (2) Å from Cu(2) is considered to be at a nonbonding distance. So, the Cu(2) environment is square pyramidal. From the stoichiometry of the compound, it was inferred that half of the copper ions are in the monovalent state and the other half in the divalent state. From the preference of copper(I) for a tetrahedral rather than a square-planar or square-pyramidal coordination geometry and also from its preference for relatively soft donor atoms, it is clear that Cu(1) is the monovalent and Cu(2) is the divalent ion. The Cu(I) ion in each asymmetric unit is connected to the Cu(II) ion in another dinuclear unit through the bridging thioether sulfur of the ligand, forming in this way tetranuclear units (see Figure 2), positioned around $^1/_4, ^1/_4, ^1/_4$. The Cu–Cu distances within this unit are Cu(1)–Cu(1′) = 5.976 (2) Å, Cu(2)–Cu(2′) = 4.278 (2) Å, Cu(1)–Cu(2′) = 3.871 (2) Å, and Cu(1)–Cu(2) = 3.073 (1) Å. These tetranuclear units are linked to one another through the rather long Cu(2) to Br(3) bonds, thereby forming a two-dimensional framework. Apart from normal van der Waals interactions, the lattice is further stabilized by a weak hydrogen bond between N(11) and Br(3) (see Table II).

The imidazole nitrogen to copper to thioether sulfur bonding angle is 81.2 (2)°. This angle is about the maximum that can be reached for this type of ligands,[24] as a result of the constraints in the "bridge". The imidazole ring is planar, with deviations from

(20) Lever, A. B. P. *Inorganic Electronic Spectroscopy*; Elsevier: Amsterdam, 1986.
(21) Prochaska, H. J.; Schwindinger, W. F.; Schwartz, M.; Burk, M. J.; Bernarducci, E.; Lalancette, R. A.; Potenza, J. A.; Schugar, H. J. *J. Am. Chem. Soc.* **1981**, *103*, 3446.
(22) Aoi, N.; Matsubayashi, G.; Tanaka, T. *J. Chem. Soc., Dalton Trans.* **1983**, 1059.
(23) Motherwell, W. D. S.; Clegg, W. PLUTO program for plotting molecular and crystal structures. University of Cambridge, England, 1978.
(24) Bouwman, E. Thesis, Leiden, 1990.

the least-squares plane of less than 0.004 Å. The copper ion lies almost in the imidazole plane with a distance of less than 0.1 Å.

Comparison with Other Structures. The compound $[Cu_2(memi)Br_3]_\infty$ combines several features in one single compound: The distinct (a) copper(I) and copper(II) ions in the mixed-valence (b) compound are held together in the tetranuclear (c) subunits by two only slightly asymmetric bromide bridges, Cu(I)–Br_2–Cu(II) (d), and two bridging thioether sulfurs, Cu(I)–S–Cu(II) (e). The tetranuclear subunits are interconnected by four Cu(I)–Br–Cu(II) bridges to a two-dimensional network (f). The copper(I) ion is in a tetrahedral SBr_3 environment (g), and the copper(II) ion is in a square-pyramidal $NSBr_3$ environment (h). Some of these features have been encountered in other compounds:

In the mixed-valence compound $[Cu^I_3Cu^{II}(\text{tetrahydrothiophene})_3Cl_5]_\infty$ the Cu(II) ion is in a flattened-tetrahedral Cl_4 environment and the Cu(I) ions are in tetrahedral S_2Cl_2 environments with the thioether sulfur bridging between two Cu(I) ions.[25]

In $[Cu^I_2Cu^{II}(CH_3SCH_2CH_2SCH_3)_6](ClO_4)_4$, a mixed-valence copper compound with coordinating thioether sulfurs,[26] discrete Cu(I) or Cu(II) ions could not be located. The compound has therefore been formulated as $[Cu(CH_3SCH_2CH_2SCH_3)_2](ClO_4)_{4/3}$. Each copper ion is coordinated by two ligands in a distorted tetrahedral geometry.

The Cu(I) and Cu(II) ions are asymmetrically bridged by two Cl^- ions in the dinuclear mixed-valence copper compound[27] $[Cu^ICu^{II}(4\text{-methylthiazole})_4Cl_3]$. The Cu(I) ion is in a distorted-tetrahedral Cl_2N_2 environment, and the Cu(II) ion is in a square-pyramidal N_2Cl_3 environment with the basal plane consisting of two thiazole nitrogens, a bridging chloride, and a terminal chloride ion and with the other bridging chloride ion at the apex.

In the dinuclear compound $[Cu(2\text{-}((tert\text{-butylthio})methyl)pyridine)Br_2]_2$, the Cu(II) ions are asymmetrically bridged by two bromide ions.[28] Each Cu(II) ion is in a distorted-square-pyramidal $NSBr_3$ environment, with the basal plane formed by the N and S donor atoms of the chelating NS ligand and by one bridging and by one terminal bromide ion, and with the apical position occupied by the other bridging bromide ion at a rather long distance (2.902 (4) Å).

The occurrence of all these features in one single compound makes the compound $[Cu_2(memi)Br_3]_\infty$ truly unique. The copper–copper distances in $[Cu_2(memi)Br_3]_\infty$ are comparable to the copper–copper distances in ascorbate oxidase. This compound could therefore be used as an EXAFS reference standard for this metalloprotein.

Redox Properties. The cyclic voltammogram of $Cu_2(memi)Br_3$ displays three subsequent redox processes in correspondence to the peak-systems A/G, B/D, and C in Figure 3. The last step has no directly associated reoxidation response in the reverse scan, except for the very far peaks E and F, which are attributable to the Cu^0/Cu^+ (stripping peak) and Cu^+/Cu^{2+} oxidations, respectively. The occurrence of peaks E and F are indicative of demetalation reactions that follow step C. An anodic current flows in all scans at the starting potential of +0.5 V. Analogously, a cathodic current is observed when the starting potential is fixed at −0.1 V. Most probably, the copper(I) center undergoes oxidation at potentials higher than $E_p(G)$, while at potentials lower than $E_p(A)$ the copper(II) center undergoes reduction, in confirmation of the mixed-valent $Cu^{II}Cu^I$ nature of the present species. Such redox steps can not be studied by voltammetric techniques at stationary electrodes; therefore, dc voltammetry at a platinum electrode with periodical renewal of the diffusion layer was used. Figure 4a shows the resulting dc voltammogram, superimposed on the relevant cyclic response. As expected, the dc voltammogram

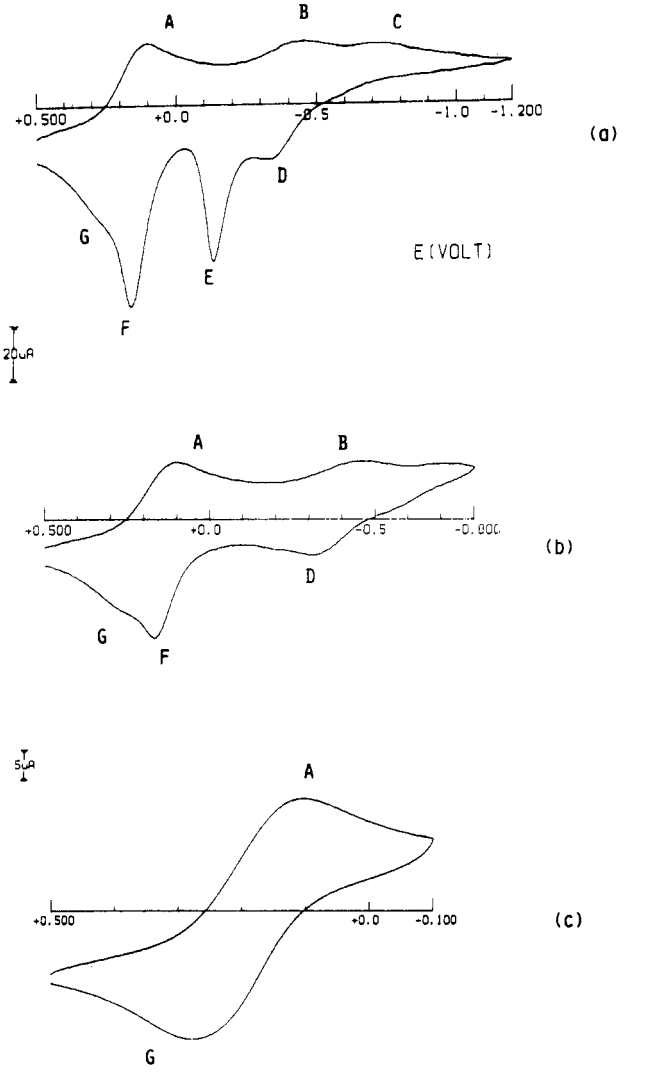

Figure 3. Cyclic voltammograms recorded at a platinum electrode on a deaerated DMSO solution containing $Cu_2(memi)Br_3$ (1.52×10^{-3} mol/dm^3) and $[NEt_4]ClO_4$ (0.1 mol/dm^3). Scan rate: 0.2 V s^{-1}. Scan ranges: (a) +500 to −1200 mV; (b) +500 to −800 mV; (c) +500 to −100 mV.

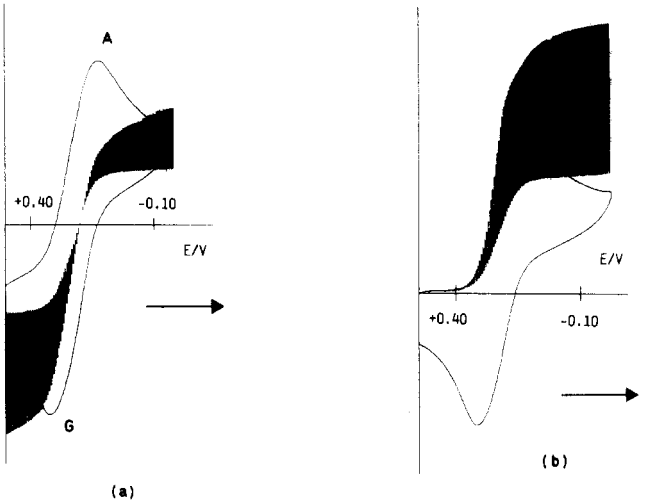

Figure 4. Dc and cyclic voltammograms recorded at a platinum electrode on a deaerated DMSO solution containing $Cu_2(memi)Br_3$ (2.65×10^{-3} mol/dm^3) and $[NEt_4]ClO_4$ (0.1 mol/dm^3): (a) initial scan; (b) scan after exhaustive one-electron oxidation at E_w = +0.5 V. Cyclic voltammetric scans at 0.2 V s^{-1}. Dc voltammetric scans at 0.02 V s^{-1}.

is constituted by a composite wave. Controlled-potential coulometric tests performed in correspondence to the anodic branch

(25) Ainscough, E. W.; Brodie, A. M.; Husbands, J. M.; Gainsford, G. J.; Gabe, E. J.; Curtis, N. F.; *J. Chem. Soc., Dalton Trans.* **1985**, 151.
(26) Olmstead, M. M.; Musker, W. K.; Kessler, R. M.; *Inorg. Chem.* **1981**, *20*, 151.
(27) Marsh, W. E.; Hatfield, W. E.; Hodgson, D. J.; *Inorg. Chem.* **1983**, *22*, 2899.
(28) Ainscough, E. W.; Baker, E. N.; Brodie, A. M.; Larsen, N. G.; *J. Chem. Soc., Dalton Trans.* **1981**, 2054.

(E_w = +0.5 V) indicated the consumption of one electron per molecule. Correspondingly, the solution turned from light green to deep green and displayed the voltammetric response shown in Figure 4b, now clearly attributable to a single-stepped two-electron reduction.

Analogously, when electrolysis of the starting mixed-valent species is performed at the potentials of the cathodic branch (E_w = −0.1 V), one electron per molecule is spent, while the solution becomes colorless. A cyclic voltammogram fully complementary to the one shown in Figure 4b results, corresponding to a single-stepped two-electron oxidation.

Analysis[29] of the cyclic voltammetric response relevant to the two-electron reduction shown in Figure 4b with scan rate v varying from 0.02 to 2.00 V s^{-1} shows that (i) the $i_p(G)/i_p(A)$ ratio is constantly equal to unity, (ii) the $i_p(A)v^{-1/2}$ term is almost constant, and (iii) the difference $E_p(G) - E_p(A) = \Delta E_p$ progressively increases from 120 to 300 mV. In addition, in dc voltammetry at 0.02 V s^{-1}, the diagnostic parameter $E(3/4) - E(1/4)$ is equal to 120 mV.

These features indicate that the mixed-valent $Cu_2(memi)Br_3$ is able to undergo a one-electron oxidation as well as a one-electron reduction at formal electrode potentials almost coincident. Both the redox changes are chemically reversible, but electrochemically quasi-reversible. For a fully reversible two-electron transfer in cyclic voltammetry, a constant ΔE_p and in dc voltammetry an $E(3/4) - E(1/4)$ of 29 mV should have resulted.

Finally, controlled-potential coulometry at potentials more negative than peak C (E_w = −1.2 V) consumes 3 faradays/mol.

All electrochemical data are consistent with the following redox scheme:

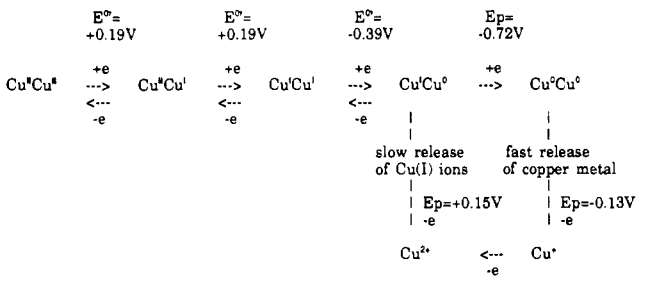

There are examples in which the two-electron reduction $Cu^{II}Cu^{II}/Cu^{I}Cu^{I}$, as well as the two-electron oxidation $Cu^{II}Cu^{II}/Cu^{III}Cu^{III}$, proceed either through a single-stepped two-electron transfer,[30-34] or through separated one-electron steps.[14,16,35-40] Chemical or electrochemical preparation of mixed-valent $Cu^{II}Cu^{I}$ species (or $Cu^{II}Cu^{III}$ species) from a $Cu^{II}Cu^{II}$ system must obviously proceed through distinct one-electron transfers. According to the described electrochemical characteristics, $Cu_2(memi)Br_3$ belongs to the valence-trapped "class I" mixed-valent species.[41] This conclusion fully agrees with the discussed X-ray structural features (vide infra) assigning Cu(1) as a monovalent copper and Cu(2) as a divalent copper. Also, the intramolecular Cu···Cu distance of 3.47 Å, even if it is not among the longest ones,[16,31] seems sufficiently long to justify the absence of direct electrostatic interactions.[35] This absence mainly[42]

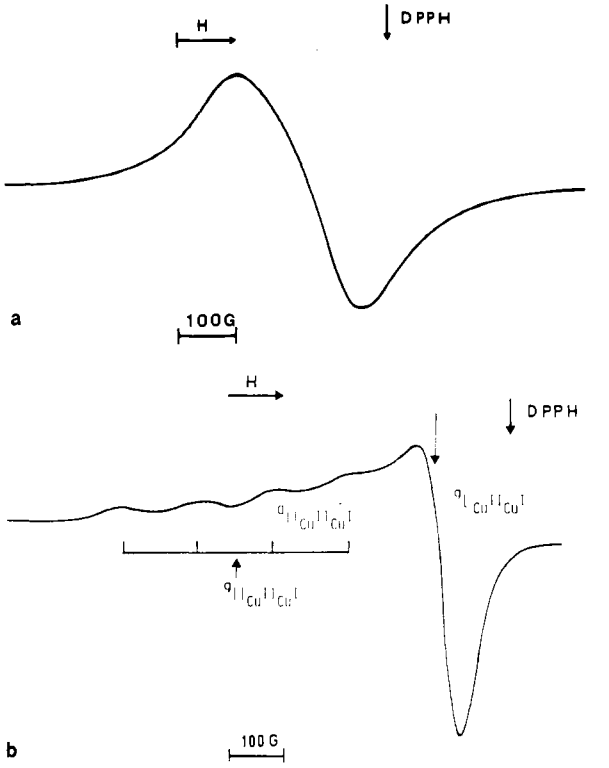

Figure 5. X-Band EPR spectrum recorded on (a) powdered $Cu_2(memi)Br_3$ and (b) a DMSO solution of $Cu_2(memi)Br_3$ (containing 0.1 M $[NEt_4]ClO_4$). T = 100 K.

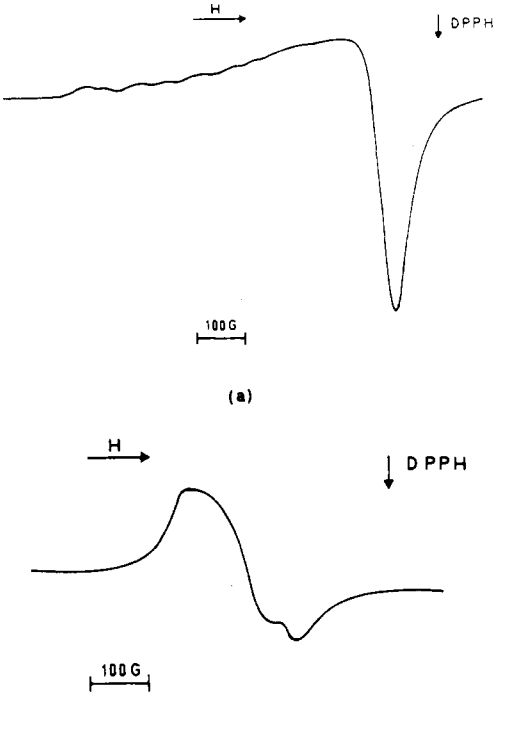

Figure 6. X-Band EPR spectra recorded on a DMSO solution of $Cu_2(memi)Br_3$ (containing 0.1 M $[NEt_4]ClO_4$) after exhaustive one-electron oxidation at +0.4 V: (a) T = 100 K; (b) T = 293 K.

(29) Brown, E. R.; Sandifer, J. *Physical Methods of Chemistry. Electrochemical Methods*, Rossiter, B. W., Hamilton, J. F., Eds.; Wiley: New York, 1986; Vol. 2, Chapter 4.
(30) Doine, H.; Stephens, F. F.; Cannon, R. D. *Inorg. Chim. Acta* **1983**, *75*, 155.
(31) Agnus, Y.; Louis, R.; Gisselbrecht, J. P.; Weiss, R. *J. Am. Chem. Soc.* **1984**, *106*, 93.
(32) Lintvedt, R. T.; Ranger, G.; Shoenfelner, B. A. *Inorg. Chem.* **1984**, *23*, 688 and references therein.
(33) Benzekri, A.; Dubordeaux, P.; Latour, J.-M.; Laugier, J.; Rey, P. *J. Chem. Soc., Chem. Commun.* **1987**, 1564.
(34) Bradbury, J. R.; Hampton, J. L.; Martone, D. P.; Maverick, A. W. *Inorg. Chem.* **1989**, *28*, 2392.
(35) Gagnê, R. R.; Kreh, R. P.; Dodge, J. A. *J. Am. Chem. Soc.* **1979**, *101*, 6917.
(36) Addison, A. W. *Inorg. Nucl. Chem. Lett.* **1976**, *12*, 899.
(37) Gagnê, R. R.; Koval, C. A.; Smith, T. J.; Cimolino, M. C. *J. Am. Chem. Soc.* **1979**, *101*, 4571.
(38) Long, R. C.; Hendrikson, D. N. *J. Am. Chem. Soc.* **1983**, *105*, 1513.
(39) Mandal, S. K.; Thompson, L. K.; Nag, K.; Charland, J. P.; Gabe, E. J. *Inorg. Chem.* **1987**, *26*, 1391.
(40) Koikawa, M.; Okawa, H.; Matsumoto, N.; Gotoh, M.; Kida, S.; Kohzuma, T. *J. Chem. Soc., Dalton Trans.* **1989**, 2089.
(41) Robin, M. D.; Day, P. *Adv. Inorg. Chem. Radiochem.* **1967**, *10*, 247.
(42) Richardson, D. E.; Taube, H. *J. Am. Chem. Soc.* **1983**, *105*, 40.

contributes to the overlapping of the $Cu^{II}Cu^{II}/Cu^{II}Cu^{I}$ and $Cu^{II}Cu^{I}/Cu^{I}Cu^{I}$ redox steps.

Comparisons of the EPR spectra in solution and in the solid state, Figure 5, afford further evidence for localized oxidation states within the dinuclear unit. The powder spectrum (Figure 5a) consists of one broad, nearly isotropic signal (ΔH_{tot} = 225 (2) G) centered at g_{av} = 2.079 (3). The second derivative temperature-dependent line shape does not give evidence to any change in spectral shape, with no appearance of hyperfine splitting. This strongly indicates the presence of remarkable magnetic coupling between the Cu(II) centers in the tetrameric unit.[43] In contrast, as expected for one unpaired electron residing on the Cu(2) atom,[36-40,44] the glassy spectrum reveals a well-resolved axial structure ($g_{\parallel} > g_{\perp}$) with the hyperfine parallel components centered at $g_{\parallel}$ = 2.342 (3) with $A_{\parallel}$ = 133 (3) G. The unresolved perpendicular absorption exhibits a relatively sharp line ($\Delta H_{\perp}$ = 70 (2) G) at $g_{\perp}$ = 2.088 (3). A g_{iso} value of 2.173 (3) can be thus computed. At room temperature the spectrum exhibits a poorly resolved line shape (ΔH_{iso} = 140 (2) G) centered at g_{iso} = 2.165 (5).

Figure 6 gives the X-band EPR spectra recorded both at liquid-nitrogen and ambient temperature on a DMSO solution of $Cu_2(memi)Br_3$ after exhaustive one-electron anodic oxidation to the corresponding $Cu^{II}Cu^{II}$ congener. The glassy spectrum is indicative of the presence of two copper(II) centers, magnetically noninteracting. It is characteristic of axial structures ($g_{\perp_{1,2}} < g_{\parallel_{1,2}}$). The line shape of the parallel region provides evidence for a "four plus four" hyperfine pattern attributable to two distinct cupric centers. The spectroscopic parameters indicate the presence of the untouched Cu(2) center ($g_{\parallel}$ = 2.346 (3), $g_{\perp}$ = 2.088 (3), $A_{\parallel}$ = 132 (3) G) together with the hyperfine parallel absorptions of the now oxidized Cu(1) center ($g_{\parallel}$ = 2.400 (3), $g_{\perp} \approx$ 2.097 (3), $A_{\parallel}$ = 116 (3) G). The calculated g_{iso} value is 2.198 (3), with a broadening of the perpendicular absorption ($\Delta H_{\perp}$ = 90 (3) G) with respect to the one of the mixed-valent precursor. The room-temperature spectrum is not resolved, but the increase in the overall linewidth (ΔH_{iso} = 185 (2) G; g_{av} = 2.160 (5)), together with the shift of the $g_{\perp}$ value in the glassy state agree with the interpretation of the spectrum as the sum of two distinct contributions from two noninteracting cupric species.

Finally, the apparent quasi-reversibility of the $Cu^{II}Cu^{II}/Cu^{II}Cu^{I}/Cu^{I}Cu^{I}$ electrochemical sequence must be considered. Departure from electrochemical reversibility may be taken as a probe for the occurrence of significant molecular reorganizations upon electron transfers.[45] However, in the case of dinuclear species, the peak-to-peak separation ΔE_p has to be related not only to the extent of electrochemical reversibility, but also to the extent of overlapping of the two one-electron transfers. On the bases of the actual data, it is hardly appropriate to speculate on the stereochemical reorganizations that will accompany oxidation to $Cu^{II}Cu^{II}$ or reduction to $Cu^{I}Cu^{I}$. Attempts to grow crystals of such congeners in order to evaluate the precise structural rearrangement accompanying these redox changes have not been successful as yet.

Acknowledgment. We gratefully acknowledge the technical assistance from ISSECC, CNR, Florence, Italy, in making susceptibility and conductivity measurements.

Registry No. $[Cu_2(memi)Br_3]_x$, 129493-04-5.

Supplementary Material Available: Tables of hydrogen atom coordinates and anisotropic thermal parameters of non-hydrogen atoms for $Cu_2(C_7H_{12}N_2S)Br_3$ (2 pages); a table of structure factors for $Cu_2(C_7H_{12}N_2S)Br_3$ (11 pages). Ordering information is given on any current masthead page.

(43) Hathaway, B. J. *Struct. Bonding* **1984**, *57*, 55.
(44) Mandal, S. K.; Thompson, L. K.; Nag, K. *Inorg. Chim. Acta* **1988**, *149*, 247.
(45) Zanello, P. *Stereochemistry of Organometallic and Inorganic Compounds*; Bernal, I., Ed.; Elsevier: Amsterdam, in press; Vol. 4, and references therein.

Contribution from the Departments of Chemistry, Abilene Christian University, Abilene, Texas 79699, and University of Missouri—Rolla, Rolla, Missouri 65401

Infrared, Magnetic, Mössbauer, and Structural Characterization of $Fe(TPP)(OReO_3)\cdot tol$ (TPP = Dianion of Tetraphenylporphyrin; tol = Toluene)

LaNelle Ohlhausen, David Cockrum, Jay Register, Kent Roberts, Gary J. Long,† Gregory L. Powell,*,‡ and Bennett B. Hutchinson*,§

Received September 14, 1989

Perrhenatoiron(III) tetraphenylporphyrin has been isolated as its toluene solvate and characterized by using magnetic susceptibility, IR and Mössbauer spectroscopy, and single-crystal X-ray diffraction. Crystal data at 20 °C are a = 12.228 (3) Å, b = 12.235 (3) Å, c = 15.968 (4) Å, α = 88.35 (2)°, β = 103.67 (2)°, γ = 113.18 (2)°, Z = 2, and space group $P\bar{1}$. The iron atom is shown to be pentacoordinate with the perrhenate ion bound in a monodentate arrangement. The average Fe–N distance is 2.059 (7) Å, and the Fe–O bond distance is 2.024 (9) Å. The toluene molecules are present at a 43° angle to the porphyrin plane. No π-bonding between the solvent and porphyrin or between porphyrin moieties is evident. Two Re–O stretching and bending vibrations at 942, 827 cm^{-1} and at 336, 321 cm^{-1}, respectively, also support the monodentate coordination of the perrhenate. The compound has a magnetic moment of 5.5 μ_B at 298 K arising from a quantum-mechanical admixture of $S = {}^5/_2$ and $S = {}^3/_2$ iron spin states in which the ${}^5/_2$ state predominates. The 78 K Mössbauer spectrum shows a quadrupole doublet with parameters consistent with this admixture, and the spectral line shape may indicate the presence of electronic relaxation between the two states on the Mössbauer time scale.

Introduction

Over the past decade, paralleling the rise in interest in metalloporphyrin chemistry, several iron(III) porphyrin compounds possessing oxyanionic ligands in the axial position have been characterized. A primary motivation for this work arose because hemoporphyrins with oxygenated ligands provide a framework for understanding important biological systems containing Fe–O bonds, and much novel coordination chemistry has been realized as well.

Solid-state structural characterization of iron(III) porphyrins with the oxyanions ClO_4^-, NO_3^-, $CH_3CO_2^-$, OR^-, SO_4^{2-}, $OTeF_5^-$, and OSO_3H^- has provided examples of monodentate, simple bidentate, and bridging bidentate coordination of the oxyanion.[1-10]

* To whom correspondence should be addressed.
† University of Missouri—Rolla.
‡ Address correspondence to this author at Abilene Christian University.
§ Address correspondence to this author at Department of Chemistry, Pepperdine University, Malibu, CA 90263.

(1) Reed, C. R.; Mashiko, T.; Bentley, S. P.; Kastner, M. E.; Scheidt, W. R.; Spartalian, D.; Lang, G. *J. Am. Chem. Soc.* **1979**, *101*, 2948.

0020-1669/90/1329-4886$02.50/0